

Abductive Action Inference

Clement Tan^{*1}, Chai Kiat Yeo^{†1}, Cheston Tan^{‡2}, and Basura Fernando^{§2}

¹Nanyang Technological University, Singapore

²Centre for Frontier AI Research (CFAR), Agency for Science, Technology and Research (A*STAR), 1 Fusionopolis Way, #16-16 Connexis, Singapore 138632, Republic of Singapore

Abstract

Abductive reasoning aims to make the most likely inference for a given set of incomplete observations. In this paper, we introduce a novel research task known as "abductive action inference" which addresses the question of which actions were executed by a human to reach a specific state shown in a single snapshot. The research explores three key abductive inference problems: action set prediction, action sequence prediction, and abductive action verification. To tackle these challenging tasks, we investigate various models, including established ones such as Transformers, Graph Neural Networks, CLIP, BLIP, GPT3, end-to-end trained Slow-Fast, Resnet50-3D, and ViT models. Furthermore, the paper introduces several innovative models tailored for abductive action inference, including a relational graph neural network, a relational bilinear pooling model, a relational rule-based inference model, a relational GPT-3 prompt method, and a relational Transformer model. Notably, the newly proposed object-relational bilinear graph encoder-decoder (BiGED) model emerges as the most effective among all methods evaluated, demonstrating good proficiency in handling the intricacies of the Action Genome dataset. The contributions of this research offer significant progress toward comprehending the implications of human actions and making highly plausible inferences concerning the outcomes of these actions.

1 Introduction

Reasoning is an inherent part of human intelligence as it allows us to draw conclusions and construct explanations from existing knowledge when dealing with an

^{*}s190099@e.ntu.edu.sg

[†]asckyeo@e.ntu.edu.sg

[‡]cheston-tan@i2r.a-star.edu.sg

[§]fernando_basura@ihpc.a-star.edu.sg

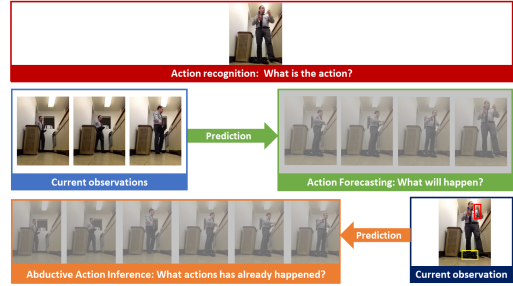


Figure 1: Different from works like action recognition (top) and action forecasting (middle), we ask the following question. Given a snapshot, what are the likely actions executed by the person before? As humans, we can infer that the person may have removed the shoes, and picked up a bottle. He may have opened the door and picked the box from the cabinet above. Even if the cabinet is partly visible, humans can derive these conclusions. This type of inference requires abductive reasoning; hence, we call this task abductive action inference (bottom).

uncertain scenario. One of the reasoning abilities that humans possess is abductive reasoning. Abductive reasoning aims to infer the most compelling explanation for a given set of observed facts. It is an extremely useful tool in our daily life, as we often rely on a set of facts to form the most probable conclusion. The ability to perform abductive reasoning about human actions is vital for human-robot collaborations. Imagine the scenario where a rescue robot enters an elderly person’s house to check on why he or she is not responding to the routine automated phone call. Upon entering the house, the robot observes its surroundings and notices that *the back door is left open but nothing else is out of the ordinary*. These observations may form a basis for a rational agent – the elderly might have *opened the door and went into the garden*. The robot can immediately make its way to search for him/her in the back

garden. In this scenario, the rescue social robot may be able to verify if the person has been safe based on the factual observations in the scene and make conclusions based on logical abduction.

In recent years, there have been some great initiatives made in abductive reasoning for computer vision. In particular, [1] generates the description of the hypothesis and the premises in natural language given a video snapshot of events. Without the generation of a hypothesis description, these methods boil down to dense video captioning. A similar task is also presented in [2] where given an image, the model must perform logical abduction to explain the observation in natural language. The use of natural language queries in these tasks presents challenges related to language understanding, making the abductive reasoning task more complicated.

In contrast to these recent works, we challenge a model to infer multiple human actions that may have occurred in the past from a given snapshot. Based on the visual information from the snapshot, objects such as a person, bottle, box, and shoes, may provide clues from which humans can draw conclusions – see Fig. 1. We term this new task, *Abductive Action Inference* and further benchmark how deep learning models perform on this challenging new task. For this task, the models are not only required to decipher the effects of human actions resulting in different environment states but also solve causal chains of action effects, a task that can be challenging even for humans. Furthermore, the task relies on the model’s ability to perform abductive reasoning based on factual evidence i.e., determining what actions may have or have not been performed based on visual information in the snapshot. Humans are able to solve this task by using prior experience (knowledge) about actions and their effects and use reasoning to make logical inferences. Are deep learning models able to perform abductive action inference by utilizing visual knowledge present in a given snapshot? We aim to answer this question in this paper.

Human action can be viewed as an evolution of human-object relationships over time. Therefore, the state of human-object relations in a scene may give away some cues about the actions that may have been executed by the human. We hypothesize that deep learning models are able to perform logical abduction on past actions using visual and semantic information of human-object relations in the scene. As these human-object relations provide substantial visual cues about actions, it makes it easier for the models to perform abductive reasoning. On the other hand, there is also the duality in which the evidence should support those conclusions (the actions inferred by the

model). If a human executed a set of actions \mathcal{A} which resulted in a state whereby a human-object relation set \mathcal{R} is formed as an effect of those executed actions (i.e., $\mathcal{A} \rightarrow \mathcal{R}$), then using the relational information, we can formulate the task by aiming to infer \mathcal{A} from \mathcal{R} . Therefore, we argue that human-object relational representations are vital for abductive action inference and provide further justifications in our experiments.

In this work, our models rely on the human-centric object relation tuples such as (person, glass) and (person, closet) obtainable from a single image at the current point in time to perform abductive action inference. One can see why these human-centric relations are vital for identifying past actions: the (person, glass) relation may lead to deriving actions such as (person-pouring-water, person-took-glass-from-somewhere) while (person, closet) may imply actions such as (person-opening-closet, person-closing-closet) see – Figure 2. Therefore, we use objects and their relationships in the scene to construct human-centric object relations within each image. These relations are made up of both visual and semantic features of recognized objects. To effectively model relational information, we use bilinear pooling and to model inter-relational reasoning, we use a new relational graph neural network (GNN). We propose a new model called BiGED that uses both bilinear pooling and GNNs to effectively reason over human-object relations and inter-relational information of a snapshot to perform abductive inference effectively. Our contributions are summarized as follows:

1. To the best of our knowledge, we are the first to propose the abductive action inference task which is different from action recognition, forecasting (see Figure 1), and language-dependent visual abductive reasoning [1, 2].
2. We benchmark several image, video, vision-language, and object-relational models on this problem, thereby illustrating the importance of human-object relational representations for the task. We also develop a new relational rule-based inference model and GPT 3.5-based relational prompt technique which serve as relevant baseline models for abductive action inference tasks.
3. Lastly, we propose a novel Relational Bilinear graph encoder-decoder model (BiGED) to tackle this challenging reasoning problem and show the effectiveness of this new design.

2 Related Work

It should be noted that our work is different from action recognition [3, 4] in a fundamental way. First, in

action recognition, the objective is to identify the actions executed in the visible data (e.g., a video or an image in still image action recognition [5]). In action recognition, the models can learn from visual cues what the action looks like and what constitutes an action. In our work, we aim to infer actions that the model has never seen the human performing. The model only sees visual evidence (e.g. human-object relations) in the scene which is the outcome of executed actions. There are no motion cues or visual patterns of actions that the model can rely on to abduct actions. From a single static image, the machine should infer what actions may have been executed. This is drastically different from classical action recognition and action anticipation tasks.

Abductive action inference has some similarity to short-term action anticipation [6,7] and long-term action anticipation [8]. However, there are several notable differences between the two tasks. Firstly, in abductive action inference, the goal of the model is to identify the most plausible actions executed by a human based on the current evidence, whereas, in action anticipation, the model learns to predict future action sequences from current observations. Next, unlike action anticipation where a short video clip is typically observed (e.g. a 2-second-long video) before predicting future actions, in abductive action inference, we only process a single snapshot (frame) to perform abductive reasoning. In addition, predictive methods [9] are mostly used for action anticipation [10], whereas in abductive action inference, we are unable to use such predictive methods during training as we only have access to a single snapshot. Furthermore, while action anticipation has to deal with the uncertainty of human behavior in the future, in abductive action inference, the evidence (objects in the scene) may suggest what actions have been executed. Additionally, in abductive action inference, the uncertainty arises from the fact that several different actions may have resulted in similar states \mathcal{R} . In our task, models should comprehend the consequences of each executed action and engage in reasoning to infer the most probable set or sequence of actions. Differences between action recognition, action forecasting, and abductive action inference are depicted in Fig 1.

Visual Commonsense Reasoning (VCR) [11, 12] is also related to our work. In VCR [11], given an image, object regions, and a question, the model should answer the question regarding what is happening in the given frame. The model has to also provide justifications for the selected answer in relation to the question. Authors in [13] also studied a similar problem where a dynamic story underlying the input image is

generated using commonsense reasoning. In particular, VisualCOMET [13] extends VCR and attempts to generate a set of textual descriptions of events at present, a set of commonsense inferences on events before, a set of commonsense inferences on events after, and a set of commonsense inferences on people’s intents at present. In this vein, given the complete visual commonsense graph representing an image, they propose two tasks; (1) generate the rest of the visual commonsense graph that is connected to the current event and (2) generate a complete set of commonsense inferences. In contrast, given a snapshot without any other natural language queries, we recognize visual objects in the scene and how they are related to the human and then use the human-centric relational representation to infer the most likely actions executed by the human.

Recently, there are machine learning models that can also perform logical reasoning. In particular, authors in [14] use abductive reasoning to improve the hypothesis of the learner. Authors in [15] showed that large language models such as ChatGPT are able to perform abductive reasoning. In particular, authors utilize the robust logical reasoning capabilities inherent in Large Language Models (LLM) to boost perception models, which are able to extract information from large unlabeled datasets. We also explored the capabilities of the GPT 3.5 turbo model for the abductive action inference task. However, our findings suggest that while GPT 3.5 is able to generate abductive inference responses, they are either overly conservative or aggressive. To address some of the limitations of existing abductive learning frameworks, authors in [16] used grounded abductive learning. This method allows us to enhance machine learning models with abductive reasoning in a ground domain knowledge base, which offers inexact supervision through a set of logic propositions [16]. We also experimented with a rule-based inference mechanism, which yields decent performance without any training. Recently, a method called abductive subconcept learning is proposed to bridge the gap between neural network learning and symbolic reasoning for unsegmented image classification [17]. In contrast to these recent works, our task involves understanding complex human behaviors, actions, and the effects of actions to reason about the state they are in and use abduction to infer the most likely actions. Furthermore, a neurosymbolic action recognition method that can generate some explanation for predicted actions is presented in [18]. Perhaps, our work is orthogonal to these ideas and our method may also benefit from these developed ideas. In VideoABC [19], models are required to infer the most plausible steps between two visual observations and provide reasons for

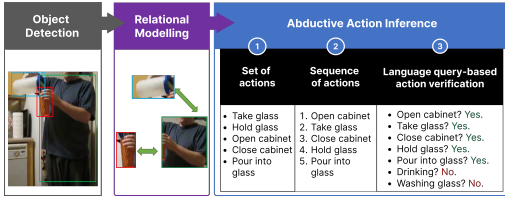


Figure 2: Proposed object-relational approach for abductive action inference. Models are tasked to: 1) abduct the set of actions, 2) abduct the sequence of actions, and 3) perform abductive action verification.

less plausible steps. Differently, we ask the model to predict the set/sequence of actions from a single snapshot and verify if an action has been executed by a human to arrive at the current snapshot.

Visual scene graph generation [20] and spatial-temporal scene graph generation [21] are also related to our work. To be specific, any advancement made in scene graph generation, in particular, modeling relations between humans and objects may also help to improve the abductive action inference task as this task heavily relies on the human-object relations to perform abduction. Furthermore, situation understanding [22] is also related to our work. Graph neural networks are also related to our work [23–25]. However, our model relies on the Jaccard Vector Similarity to construct the affinity of the nodes and employs an encoder-decoder model. Our work is also related to bilinear pooling methods such as [26, 27]. However, we utilize bilinear pooling for relational modeling and abductive action inference. Visual reasoning methods such as [28, 29] are also related to our work. However, our main focus is to investigate whether deep learning models are able to perform abductive reasoning. Unlike visual question answering, our reasoning task does not involve language.

3 Abductive Action Inference

Task: Given a single snapshot, models have to infer the actions executed by the human up to the current moment in time using abductive reasoning which we coined Abductive Action Inference. Let us denote a human action by $a_i \in A$ where A is the set of all actions and E_1, E_2, \dots is a collection of evidences from the evidence set \mathcal{E} . As the evidence is a result of actions, we can write the logical implication $\mathcal{A} \rightarrow \mathcal{E}$ where \mathcal{A} is the set/sequence of actions executed by a human which resulted in a set of evidence \mathcal{E} . Then, the abductive inference task aims to derive 1) the set of actions, 2) the sequence of actions that resulted in the current

evidence shown in the image, and 3) abductive action verification. In abductive action verification, the model is given a single snapshot and is required to answer a binary yes/no to an action query (did the person execute action a_x ?).

We benchmark three approaches to solve these tasks, 1) end-to-end trained models such as Slow-Fast networks [30], 2) vision-language models such as CLIP [31], BLIP [32], and 3) object-relational reasoning models. In the following subsections, we outline the details of the object-relational reasoning models and end-to-end training and vision-language models in the experiments section. We also provide the details of abductive action set/sequence prediction, and verification using the object-relational approach.

3.1 Object-Relational Representation Approach

Our primary hypothesis is that human-object relations are essential for abductive action inference. Therefore, we propose a human-object relational approach for the task. In all three tasks, our general approach is as follows. We make use of detected humans and objects in the snapshot and then generate a representation for human-centric object relations. Then, using these human-centric object relations, we summarize the visual snapshot, and using neural models, we infer the most likely actions executed by the human. The overview of this approach is shown in Figure 2. Next, we first discuss abductive action set inference, followed by the details of abductive action sequence inference and abductive action verification.

Abductive action set prediction Let us denote the object by $o \in O$, the predicate category by $p \in P$, and the human by h . The j^{th} relation R_j is a triplet of the form $\langle h, p, o \rangle$. In the i^{th} snapshot, we observe n number of relations $\mathcal{R}_i = \{R_1, R_2, \dots R_n\}$ where \mathcal{R}_i is the relation set present in the situation shown in that snapshot. These relations constitute the evidence (\mathcal{E}). The relation set \mathcal{R}_i is an effect of a person executing an action set/sequence $\mathcal{A}_i = \{a_1, \dots a_K\}$. Therefore, the following association holds.

$$\mathcal{A}_i \rightarrow \mathcal{R}_i \quad (1)$$

However, we do not know which action caused which relation (evidence), as this information is not available. The association reveals that there is a lack of specific knowledge about the exact effects of individual actions and when multiple actions have been executed, the resulting effect is a combined effect of all executed actions. Consequently, the learning mechanism must un-

cover the probable cause-and-effect relationships concerning actions. Therefore, given \mathcal{R} we aim to perform abductive action inference to infer the most likely set of actions executed by the human using neural network learning.

We learn this abduction using the deep neural network functions $\phi()$, and $\phi_c()$ of the following form by maximizing the conditional probability of actions given the relational evidence as follows:

$$x_r = \phi(R_1, \dots, R_n; \theta_\phi) \quad (2)$$

$$P(a_1, \dots, a_K | R_1, \dots, R_n) = \phi_c(x_r; \theta_c) \quad (3)$$

where ϕ is the relational model that outputs a summary of relational information as a vector x_r . Here, ϕ_c is the linear classifier (or predictor) having the parameters θ_c and the parameters of the relational model are denoted by θ_ϕ . The training and inference sets comprise snapshots (images) and corresponding action set \mathcal{A}_i . From each snapshot, we extract the relation set \mathcal{R}_i . Therefore, the dataset consists of $\mathcal{D} = \bigcup_i \{\mathcal{R}_i, \mathcal{A}_i\}$. Given the training set (\mathcal{D}), we learn the model function in Equations 2 and 3 using backpropagation as follows:

$$\theta_\phi^*, \theta_c^* = \underset{\theta_\phi, \theta_c}{\operatorname{argmin}} \sum_i -\log(P(\mathcal{A}_i | \mathcal{R}_i)) \quad (4)$$

where $\theta_\phi^*, \theta_c^*$ are the optimal parameters. As this is a multi-label-multi-class classification problem, we utilize the max-margin multi-label loss during training.

Abductive action sequence prediction To generate the sequence of actions, we use the relational model $\phi()$, output x_r , and the classifier output $\phi_c()$ and utilize a sequence decoder (GRU or Transformer) to generate the sequence of actions using element-wise cross-entropy loss during training. More details are given in section 4.9. Interestingly, this task requires the model to resolve causal chains of action effects when abducting the sequence of actions. Thus, this task is more challenging than action set prediction.

Abductive action verification Abductive verification model $\phi_{ver}()$ takes the evidence \mathcal{E} and the semantic representation of the action (e.g. textual encoding of the action name) y_a as inputs and outputs a binary classification score indicating if the evidence supports the action or not, i.e. $\phi_{ver}(\mathcal{E}, y_a) \rightarrow [0, 1]$. Specifically, we encode the action name using the CLIP [31] text encoder to obtain the textual encoding y_a for action class a . Then, we concatenate y_a with x_r and utilize a two-layer MLP to perform binary classification to determine whether action a was executed or not. We use the max-margin loss to train $\phi_{ver}()$.

3.2 Relational Representation

To obtain the relation representation, we extract features from the human and object regions of each snapshot (image) using a FasterRCNN [33] model with a ResNet101 backbone [34]. Let us denote the human feature by x_h , the object feature by x_o , and the features extracted from taking the union region of both human and object features by x_u . As we do not know the predicate or the relationship label for the relation between x_h and x_o , we use the concatenation of all three visual features x_h, x_o , and x_u as the joint relational visual feature $x_v = [x_h, x_o, x_u]$. Using FasterRCNN, we can also obtain the object and human categories. We use Glove [35] embedding to acquire a semantic representation of each human and object in the snapshot. Let us denote the Glove embedding of the human by y_h and the object by y_o . Then, the semantic representation of the relation is given by $y_s = [y_h, y_o]$. Using both visual and semantic representations, we obtain a joint representation for each human-centric relation in a given snapshot. Therefore, the default relation representation for a relation $R = \langle h, p, o \rangle$ is given by $r = [x_v, y_s]$. Note that we do not have access to the predicate class or any information about the predicate. Next, we present several neural and non-neural models that we developed in this paper that uses relational representations for the abductive action inference task.

3.3 GNED: Relational Graph Neural Network

In our work, the graph neural network-based encoder-decoder model summarizes relational information for abductive action inference. Given the relational data with slight notation abuse, let us denote the relational representations by a $n \times d$ matrix $\mathcal{R} = [r_1, r_2, \dots, r_n]$ where r_n has d dimensions. In our graph neural network encoder-decoder (GNED) model, we first project the relational data using a linear function as follows:

$$\mathcal{R}' = \mathcal{R}W_l + b_l \quad (5)$$

where $\mathcal{R}' = [r'_1, r'_2, \dots, r'_n]$. Then, we construct the affinity matrix $W_A(i, j)$ using Jaccard Vector similarity, where $W_A(i, j)$ shows the similarity/affinity between the i -th relation and the j -th relation in the set. Here, we use Jaccard Vector Similarity which is a smooth and fully differentiable affinity [7]. Note that Jaccard Vector Similarity is bounded by $[-1, 1]$. Therefore, we obtain the graph-encoded relational representation as follows:

$$G_e = \operatorname{ReLU}((W_A \mathcal{R}')W_g + b_g) \quad (6)$$

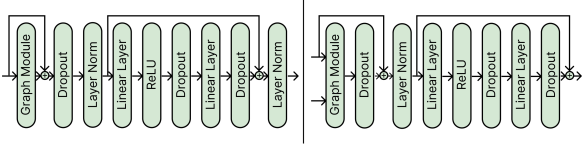


Figure 3: The graph neural network encoder (left) and graph neural network decoder (right) architecture. The residual connections are shown with the + sign.

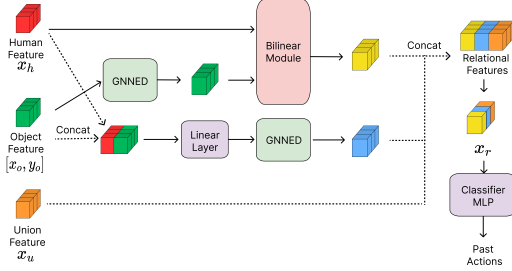


Figure 4: The Bilinear Graph Encoder-Decoder (BiGED) architecture.

where W_g and b_g are the weight matrix and bias term respectively. We call equations 5-6 the graph module. Using the graph module as a base model, we develop a graph encoding layer. The relational graph neural network encoder-decoder architecture we proposed is shown in Figure 3. Our graph encoder-decoder model consists of one graph encoder and three graph decoders by default. The graph module is able to model the inter-relations between human-object relations and reasons about them to perform abduction on actions. The graph encoding layer (left) is very similar to the Transformer encoder layer [36]. The graph encoding layer consists of drop-out layers, layer norm [37], linear layers, and residual connections [34]. The graph decoder layer (right) is also similar to a Transformer decoder layer except for the graph module. Finally, we apply max-pooling at the end of the graph encoder-decoder model to obtain the final snapshot representation x_r .

3.4 RBP: Relational bilinear pooling

To effectively model the higher-order relational information between human and object features, we use bilinear pooling. Given the human representation x_h and the object representation x_o , we use bilinear pooling with a weight matrix W_b of size $d \times d \times d$ and linear

projection matrices W_{bl}, W_{jb} as follows:

$$o' = \text{ReLU}(W_o x_o + b_o) \quad (7)$$

$$h' = \text{ReLU}(W_h x_h + b_h) \quad (8)$$

$$r_b = \text{ReLU}([h'W_b o'; ([h'; o']W_{bl} + b_{bl})])W_{jb} + b_{jb} \quad (9)$$

where $[\cdot]$ represents the vector concatenation and $h'W_b o'$ is the bilinear pooling operator applied over human and object features. $([o'; h']W_{bl} + b_{bl})$ is the output of concatenated human and object features followed by a linear projection using weight matrix W_{bl} and bias term b_{bl} . In contrast to bilinear pooling, the concatenated linear projection captures direct relational information between human and object features. Then, we concatenate the bilinear pooled vector $(h'W_b o')$ and the output of the linear projection $([o'; h']W_{bl} + b_{bl})$. Next, we use ReLU and apply another linear projection $(W_{jb} + b_{jb})$. Finally, we concatenate the overlap feature x_u with the overall model output (r_b) and apply max-pooling across all relational features $([r_b; x_u])$ in the image to obtain x_r .

3.5 BiGED: Bilinear Graph Encoder-Decoder

Finally, to take advantage of both bilinear relational modeling and graph neural network encoder-decoder models, we combine both strategies as shown in Fig 4. The main idea is to replace the projection function in Equation 7 with a graph neural network encoder-decoder model. Let us denote the graph neural network encoder-decoder model by $f_{Ged}()$. Then, equation 7 will be replaced as follows:

$$O' = f_{Ged}(X_o) \quad (10)$$

where X_o is all the object features in the snapshot. Afterward, we apply equation 9 before using bilinear modeling to obtain the relational representation. Note that as there are only one or two humans in the snapshot, we do not use the GNNED to model human semantic features. The inputs to the BiGED model are the visual human features x_h , concatenated visual and semantic object features $[x_o, y_o]$ as well as the union features x_u . Next, we concatenate the human and object features $[x_h, x_o, y_o]$ to obtain a joint feature and then pass it through a linear layer and another GNNED model. The outputs of the bilinear, joint feature-based GNNED models and overlap union feature x_u are concatenated to obtain the final relational representation. Afterward, we use max-pooling to obtain the representation x_r for the snapshot. For all models, we employ a linear classifier to infer past actions using the representation vector x_r .

3.6 Rule-based abductive inference

In abductive action inference, we assume the following logical association holds,

$$\{a_1, a_2, a_3, \dots, a_K\} \rightarrow \{R_1, R_2, \dots, R_N\} \quad (11)$$

where $\{R_1, R_2, \dots, R_N\}$ is the relation set \mathcal{R} present in a snapshot and $\{a_1, a_2, a_3, \dots, a_K\}$ is the action set \mathcal{A} executed by the human to arrive at the snapshot. Note the set of all actions is denoted by A where $\mathcal{A} \subset A$.

In rule-based inference, each relation is in the symbolic form $R_k = \langle H, o_k \rangle$ where H and o_k are the human feature and k^{th} object label in the snapshot. As the human feature is common in all relations, we omit the human feature in each relation. Then, the relational association is updated as follows:

$$\{a_1, a_2, a_3, \dots, a_K\} \rightarrow \{o_1, o_2, \dots, o_N\} \quad (12)$$

for any snapshot. In rule-based abductive action set inference, for each given object pattern $\{o_1, o_2, \dots, o_N\}$, we count the occurrence of each action a_j . Let us denote the frequency of action a_j for object pattern $\mathcal{O}_q = \{o_1, o_2, \dots, o_N\}$ from the entire training set by C_j^q . Therefore, for each object pattern \mathcal{O}_q , we obtain a frequency vector over all actions denoted by:

$$\mathbf{C}^q = [C_1^q, C_2^q, \dots, C_{|A|}^q] \quad (13)$$

Then, we can convert these frequencies into probabilities using softmax:

$$P(A|\mathcal{O}_q) = \text{softmax}([C_1^q, C_2^q, \dots, C_{|A|}^q]) \quad (14)$$

We use this to perform abductive action set inference using the test set. Given a test snapshot, we first obtain the object pattern \mathcal{O} . Next, we obtain the action probability vector for the object pattern from the training set using Equation 14. If an object pattern does not exist in the training set, we assign equal probability to each action.

3.7 Relational GPT 3.5 abductive inference

GPT and later versions [38–40] have revolutionized the AI field by solving many natural language processing and reasoning tasks. Here, we use the GPT 3.5 turbo version to perform abductive action inference. To do this, we generate a query prompt as well as a contextual description for each snapshot using the ground truth relational annotations based on the subject-predicate-object triplet relation. In contrast to the aforementioned methods, we utilize the ground truth predicate

person is sitting on sofa/couch, person is not looking at sofa/couch, person is behind sofa/couch, person is sitting on chair, person is not looking at chair, person is beneath chair, person is holding cup/glass/bottle, person is looking at cup/glass/bottle, person is in front of cup/glass/bottle	I need to know what actions person executed to arrive in the state explained in the context. Select subset of action numbers between [1] and [157]. [1] = Holding some clothes, [2] = Putting clothes somewhere, [3] = Taking some clothes from somewhere, [4] = Throwing clothes somewhere, ... [157]
Context	Prompt

Figure 5: The context description and the textual prompt used for the GPT 3.5 turbo model.

label for GPT3.5. An example of the contextual description and textual prompt is shown in Figure 5. In addition, an answer generated by GPT3.5 is shown in Figure 6. We specifically created the prompt such that GPT3.5 responses are constrained to the ground truth action sets within the dataset. Based on the responses from the GPT3 model, we construct the score vector where the predicted action is marked with a score of 1 or 0 otherwise. We call this hard matching as we add 1 if and only if the GPT model outputs the exact action class name given in the input prompt.

GPT 3.5 + CLIP (Text): Occasionally, the GPT3.5 model generates answers not limited to the specified action classes in the prompt. To solve this problem, we use a soft matching technique using the CLIP text encoder [31]. We encode the ground truth class name for class a using the CLIP text encoder to obtain a vector $y_a \in R^{1 \times d}$. Similarly, we obtain a CLIP text vector for each response from the GPT 3.5 model. If there are n numbers of GPT 3.5 responses, then we obtain n vectors $T = [t_1, \dots, t_n]$ where $t_n \in R^{1 \times d}$. We then take the dot product and apply an average of softmax as the score of the snapshot as follows:

$$\text{score} = \frac{1}{n} \sum_j \text{softmax}(Y_a \cdot t_j^T) \quad (15)$$

where Y_a is the CLIP class encoding matrix for all classes. Finally, these soft scores are added to the hard scores.

3.8 Relational MLP

The MLP consists of 2-layers. The human feature x_h , object feature x_o , and union region of both human and feature x_u obtained from the ResNet-101 FasterRCNN backbone are concatenated to form the joint relational visual features x_v . The semantic representation y_s is formed via a concatenation of the Glove [35] embedding of the human y_h and object y_o . We perform max

<p>person is leaning on window, person is looking at window, person is on the side of window, person is holding food, person is not looking at food, person is in front of food, person is holding dish, person is not looking at dish, person is in front of dish, person is holding sandwich, person is not looking at sandwich, person is in front of sandwich,</p>	<p>Based on the context provided, the actions executed by the person are as follows:</p> <p>[90] = Opening a window [93] = Watching/Looking outside of a window [62] = Holding some food [68] = Holding a sandwich [119] = Holding a dish</p>	<p>Holding some food Holding a sandwich Watching/Looking outside of a window Drinking from a cup/glass/bottle Holding a dish</p>
Context	GPT Answer	Ground truth

Figure 6: Answer generated by GPT 3.5 model. The correct answers are shown in green color whereas false positives and negatives are shown in red.

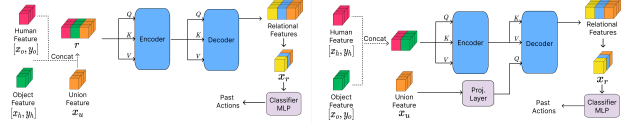


Figure 7: (left) The relational multi-head self-attention Transformer. (right) The relational cross-attention Transformer.

pooling on the relational features, $\mathcal{R}_i = r_1, r_2, \dots, r_n$ in a given snapshot, where each $r_n = [x_v, y_s]$ is the concatenation of visual and semantic features. Afterward, we pass these features into the 2-layer MLP. The inputs and outputs of the first layer are D-dimensional and we apply dropout with $p = 0.5$. The last layer of the MLP is the classification layer. Lastly, we apply a Sigmoid function before applying multi-label margin loss to train the model.

3.9 Relational Transformer

Transformers [36] are a popular class of models in deep learning. They are effective at capturing relationships between far-apart elements in a set or a sequence. In this work, we use Transformers as a set summarization model.

Multi-head self-attention Transformer: Specifically, we utilize a multi-head self-attention (MSHA) Transformer model. The MSHA Transformer contains one encoder and three decoder layers by default. We do not use any positional encoding as we are summarizing a set. Given the set of relational representation of an image $\mathcal{R}_i = r_1, r_2, \dots, r_n$, the Transformer model outputs a Tensor of size $n \times d$ where d is the size of the relational representation. Afterward, we use max-pooling to obtain a snapshot representation vector x_r . A visual illustration of this model is shown in Fig. 7 (left).

Cross-attention Transformer model: Similar to the multi-head self-attention Transformer, we use one encoder and three decoder layers. The inputs to

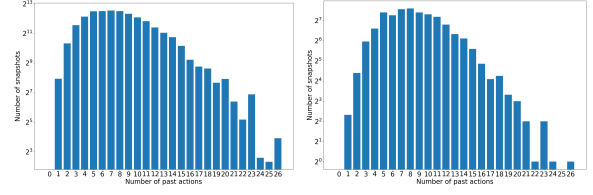


Figure 8: Number of snapshots (in \log_2) for sets of n past actions in the Action Genome test set. (a) – *Abduct at T*, (b) – *Abduct last snapshot*

the Transformer encoder are the concatenation of the human and object visual and semantic features $[x_h, y_h, x_o, y_o]$ excluding union features x_u . During the decoding, the Transformer decoder takes the union region visual feature of both human and object x_u as the query and the output of the Transformer encoder as the key and the values respectively. We have ablated many different versions of Cross-attention and we found this particular architecture performs the best. This model is shown in Fig. 7 (right).

4 Experiments and Results

4.1 Dataset: Action Genome Abductive Inference dataset

We extend the Action Genome (AG) dataset [41] and benchmark all models on the AG dataset for the Abductive Action Inference task. Built upon the Charades dataset [42], the AG dataset contains 9,848 videos with 476,000+ object bounding boxes and 1.72 million visual relationships annotated across 234,000+ frames. The original objective of this dataset is to study spatial-temporal scene graph generation. *It should be noted that not all video frames in the Charades dataset are used in the AG dataset. Only a handful of key frames are used in AG, and we follow the same.* The AG dataset does not provide action annotations. To obtain action annotations for snapshots of AG, we leverage the Charades dataset which contains 157 action classes. To be specific, we use frame-level action annotations from Charades to get the action annotations for AG snapshots. Then, we construct the training and testing dataset for abductive action inference. Next, we describe the process of generating action sets and sequences using the images from the Action Genome and action labels from the Charades dataset for the abductive inference task.

How to generate action sets and sequences? To obtain the ground truth action set \mathcal{A} for a snapshot in the Action Genome dataset using the Charades action

labels, we first compute the time t for each individual frame within a video sequence by using the formula: $t = \frac{v_d}{n}$, where v_d and n denote the video duration and the number of frames in the video respectively. Then, we multiply the current frame number f_n with t to obtain the current time, $t_c = t \times f_n$.

Action sets: As each video contains multiple actions, we check whether the current time of the frame t_c , falls within the start t_s and end t_e time of the action. If it does, we add the ground truth action label to the action set \mathcal{A}_n for the snapshot. To obtain the ground truth action set for the t^{th} snapshot, we combine all previous action sets from $t = 1$ up to and including the t^{th} snapshot to form the set.

Action sequences: We sort the start time t_s of the actions contained in the video in ascending order. Then, for each snapshot, if the current time of the frame is greater than the start time of the action ($t_c \geq t_s$), we add it to the sequence.

4.2 Experimental Setup

After obtaining the action annotations of snapshots for a given video, we drop videos having only one snapshot as there are no past snapshots and therefore, no past actions. For the remaining snapshots, we assign action labels from the previous snapshots in two different evaluation setups:

1. Abduct at T : Given a snapshot at time T , we add action labels from all the previous snapshots (frames) to the ground truth (including actions from the current snapshot) where \mathcal{A}_t denotes all actions of the t^{th} snapshot. Therefore, the ground truth action set \mathcal{A} is given by $\mathcal{A} = \bigcup_{t=1}^T \mathcal{A}_t$.

2. Abduct last snapshot: Based on the first setup, we add an additional task where the model has to perform inference only on the last snapshot of each video which contains all past actions. If the last snapshot is T' , then the action set is $\mathcal{A} = \bigcup_{t=1}^{T'} \mathcal{A}_t$. Note that in the Action Genome dataset, the snapshots are sampled non-homogeneously from the Charades dataset videos. Therefore, the previous snapshot occurs several seconds before the current snapshot. In our abductive action inference task, the ground truth action sets are confined to the length of each video. We provide details on the number of snapshots for a set of n past actions in the AG dataset for these setups in Figure 8. As can be seen from these statistics, the majority of the snapshots have more than five actions and some snapshots have as many as 26 actions.

4.3 Evaluation Metrics

We utilize the mean Average Precision (mAP), Recall@K (R@K), and mean Recall@K (mR@K) metrics to evaluate the models for the abductive action set prediction and action verification tasks. Each snapshot contains 8.9 and 8.2 actions for the **Abduct at T** and **Abduct last snapshot** setups respectively. Therefore, K is set to 10 based on the average number of actions contained in a snapshot. Lastly, we use the Hamming Loss to evaluate the action sequence prediction models as follows:

$$H = \frac{1}{N * L} \sum_{n=1}^N \sum_{l=1}^L [y_l \neq \hat{y}_l] \quad (16)$$

where N is the total number of samples and L is the sequence length. Finally, for a given sample, the accuracy is $(1 - H) \times 100$.

4.4 Implementation Details

We use FasterRCNN [33] with a ResNet101 [34] backbone to extract human and object features from each snapshot based on the ground truth person and object bounding boxes provided by AG for all object-relational models. We load pre-trained weights provided by [21] that were trained on the training set of AG which obtained 24.6 mAP at 0.5 IoU with COCO metrics. The parameters of the FasterRCNN during training and inference are fixed for the abductive action inference task. Our default human and object visual representations have 512 dimensions obtained from 2048 dimensional visual features from the FasterRCNN. We use linear mappings to do this. During training, we train the models for 10 epochs and set the batch size to 1 video (there are many frames in a video). We assume the frames are i.i.d. Note that even though there are multiple snapshots in a batch, the snapshots are processed in parallel and individually for the transformer and graph models respectively. There is no sharing of information between snapshots. We use the AdamW [43] optimizer with an initial learning rate of 1e-5 along with a scheduler to decrease the learning rate by a factor of 0.5 to a minimum of 1e-7. We utilize Glove [35] word embedding of size 200 for object and subject (human) semantic features. In addition, gradient clipping with a maximal norm of 5 is applied. Moreover, we report the mean across 3 different runs for each configuration to ensure we report the most accurate performance of our models. All models (except end-to-end) are trained on a single RTX3090 or A5000 GPU. For CLIP, we use publicly available implementations [31]. We use the public API of OpenAI for GPT 3.5 models.

4.5 Baseline Models

We benchmark several publicly available image (Resnet101-2D, ViT [44]) and video models (Slow-Fast [30] and Resnet50-3D) using their official implementations. Image models are pre-trained on ImageNet [45] while video models are pre-trained on Kinetics400 [46] dataset and we fine-tune these models on our task. We use a batch size of 32 with a learning rate of 1e-5 for ResNet and Slow-Fast networks. As for ViT, we use a batch size of 2042. For video-based methods, we select the surrounding 8 frames of a snapshot from the Charades dataset to fine-tune these models end-to-end. We also use CLIP linear-probe and zero-shot to perform abduction using several variants of the CLIP model [31]. We also evaluate the BLIP [32] model using question answering (inference with generate option) on this task. We also benchmark against an action anticipation model that correlates past observations with the present [7]. Furthermore, we evaluate the reasoning capabilities of gpt-3.5-turbo [40] for this task.

4.6 Human Performance Evaluation

We report the human performance on the abductive action inference set, sequence, and verification tasks for the *Abduct at T* setup in Tables 1, 3, and 4. All human experiments for the three sub-problems based on the *Abduct at T* setup are executed in the same manner. First, we randomly sample 100 test snapshots and ask evaluators to manually go through every action class in the Charades dataset without looking at the ground truth for each snapshot. Then, evaluators select the set of actions that are likely to have occurred before the snapshot. Next, depending on the task, we compute the evaluation metrics outlined in the previous section.

4.7 Evaluation of Abductive Action Set Prediction

Our results for the abductive action inference set prediction task are shown in Table 1. These results are obtained based on the *Abduct at T* setup. During training, the model learns from every single snapshot in the video sequence independently. Likewise, during inference, the model predicts the past action set on every single snapshot. The end-to-end trained models such as Slow-Fast [30], ResNet50-3D, Resnet101-2D, and ViT perform poorly as it may be harder for these models to find clues that are needed for the abductive inference task. As there are no direct visual cues to infer previous actions (unlike object recognition or action recognition) from a given snapshot, end-to-end learning becomes harder or near impossible for these models.

Table 1: Abductive action set inference performance using the proposed methods on the *Abduct at T* setup.

Model	mAP	R@10	mR@10
Human Performance	-	80.60	82.81
End-to-end training			
Slow-Fast [30]	7.91	14.42	7.65
ResNet101-2D [34]	9.27	18.63	11.51
Resnet50-3D [30]	8.16	16.08	7.83
ViT B/32 [44]	7.27	16.84	8.82
Vision-language models			
CLIP-ViT-B/32 (zero-shot) [31]	14.07	14.88	20.88
CLIP-ViT-L/14 (zero-shot) [31]	19.79	21.88	27.77
CLIP-ViT-B/32 (linear probe) [31]	16.16	31.25	16.38
CLIP-ViT-L/14 (linear probe) [31]	22.06	40.18	20.01
BLIP (vqa) [32]	6.18	9.84	15.76
Object-relational methods - using gt human/objects			
GPT 3.5	9.98	25.22	20.32
GPT 3.5 + CLIP (Text)	13.01	25.56	23.21
Relational Rule-based inference	26.27	48.94	36.89
Relational MLP	27.73	42.50	25.80
Relational Self Att. Transformer	33.59	56.03	40.04
Relational Cross Att. Transformer	34.73	56.89	40.75
Relational GNNED	34.38	57.17	42.83
Relational Bilinear Pooling (RBP)	35.55	59.98	43.53
Action Anticipation [7]	34.41	53.40	41.84
BiGED	35.75	60.55	44.37
Object-relational method - using FasterRCNN labels			
BiGED	24.13	43.59	30.12

Table 2: Abductive action set inference performance using the proposed methods on the *Abduct last snapshot* setup.

Model	mAP	R@10	mR@10
Relational Rule-based inference	26.18	44.34	33.94
Relational MLP	25.99	38.79	23.54
Relational Self Att. Transformer	30.13	47.55	35.05
Relational Cross Att. Transformer	31.07	48.33	35.32
Relational GNNED	30.95	48.18	36.36
RBP	31.48	49.79	36.96
BiGED	31.55	49.62	36.15

On the other hand, multi-modal foundational models such as the CLIP [31] variants are able to obtain better results than vanilla CNN models on this task perhaps due to the quality of the visual representation. Interestingly, object-relational models such as MLP and rule-based inference obtain decent performance. One might argue that the performance of human-object relational models is attributed to the use of ground truth object labels in the scene. However, when we tried to incorporate ground truth objects in the CLIP [31] model, performance was poor as well. Therefore, we conclude that the CLIP and BLIP models without any further modifications are not suited for abductive action inference. The poor performance of the models, CLIP and BLIP, might be attributed to their training approach, which aims to align overall image features with corresponding text features. During their training, both CLIP and BLIP assume that the text in the captions accurately describes the visual content of the image. However, when it comes to abductive action inference, there are no explicit visual cues available to indicate the execution of certain actions. We also note

that the CLIP model demonstrates reasonable zero-shot performance. This may be due to the fact that better vision features are learned by the CLIP model.

The GPT model is able to generate reasonable answers in some snapshots (see Fig 6). However, most of the time GPT answers are either overly conservative or aggressive. For example, GPT responds *”There is not enough information given in the context to determine the specific actions the person executed to arrive in the described state”* and in some instances, it selects all action classes. This may be the main reason for the poor performance of GPT. However, it should be noted that the GPT model is fed with more information than all other baselines as we also provide the predicate relation to the GPT 3.5 model. We also note that the GPT 3.5 + CLIP (Text) model with both soft and hard scores performs better than the hard score method. Assuming that large language models such as GPT 3.5 are capable of human-like reasoning, we can perhaps suggest that abductive inference requires more than text-based reasoning and commonsense reasoning. Given the fact that pure rule-based inference performs better than GPT 3.5 with lesser information may suggest that GPT 3.5 is not suited for abductive action inference due to it not having a detailed understanding of some of the human behaviors and effects of human actions.

The results also suggest that the human-object relational representations provide valuable evidence (cues) about what actions may have been executed in contrast to holistic vision representations. Among object-relational models, the MLP model and rule-based inference perform the worst across all three metrics. The rule-based inference does not use any parametric learning and therefore it can only rely on statics. Interestingly, the rule-based method obtains similar performance to the MLP model indicating the MLP model merely learns from the bias of the dataset.

The Relational Transformer model improves results over MLP. Furthermore, the Relational GNNED performance is comparable to the Relational Transformers. The Transformer variants and GNNED have similar architectural properties and have better relational modeling capacity than the MLP model. These models exploit the interrelation between visual and semantic relational representations to better understand the visual scene. This potentially helps to boost the performance of abductive action inference.

Surprisingly, Relational Bilinear Pooling (RBP) obtains particularly good results outperforming the Transformer and GNNED models. The way relational reasoning is performed in RBP is fundamentally different from Transformers and GNNED. The RBP mod-

Table 3: Abductive action sequence prediction using the proposed methods on the *Abduct at T* setup.

Model	Accuracy	
	GRU	Transformer
Human performance	14.00	
Relational MLP	9.43	9.59
Relational Self Att. Transformer	9.71	9.95
Relational Cross Att. Transformer	9.69	9.96
Relational GNNED	9.81	10.11
RBP	10.48	10.22
BiGED	10.54	10.15

els interactions between the human and object features within a relation more explicitly than the GNNED and Transformer. However, unlike the GNNED or Transformer, RBP is unable to model interactions between relations. Finally, the combination of GNNED and RBP, i.e., BiGED performs even better. This result is not surprising as BiGED takes advantage of better inter and intra-relation modeling.

An action anticipation model that correlates past observations with the future [7] also performs well using relational features. However, this model has access to prior snapshots during training which other models did not use. All object-relational models utilize the ground truth object labels from the AG dataset to obtain semantic representations. We observe a drop in performance when we use predicted objects from the FasterRCNN model. Nevertheless, the performance of BiGED with FasterRCNN labels is significantly better than end-to-end trained models and vision-language models. Finally, it should be emphasized that human performance on this task is significantly better than any of the modern AI models.

4.8 Evaluation of abduction on the last snapshot

Next, we evaluated the performance of object-relational models on the second setup where the model has to *perform abduction on the last snapshot of each video*. However, we only focus on object-relational methods. To be specific, we use the trained models in the previous setup directly for inference. As a myriad of actions could have happened throughout a video sequence, this setup is particularly challenging. The results of this task are shown in Table 2. We observe that the results are lower than the previous setup for all models, demonstrating that the task is more challenging. The MLP model and the rule-based inference have relatively poor performance. Similar to the previous setup, the GNNED, RBP, and BiGED methods outperform the Transformer model even though the GNNED shares a similar architecture to the Transformer. Although the BiGED obtains the best performance for mAP, we note that the best-performing

Table 4: Abductive action verification performance using the proposed methods on the *Abduct at T* setup.

Model	mAP	R@10	mR@10
Human Performance	–	92.26	93.71
Relational MLP	26.58	41.71	25.40
Relational Self Att. Transformer	27.94	45.72	30.12
RBP	32.19	53.76	38.44
BiGED	34.13	57.39	41.97

model for R@10 and mR@10 is the RBP model.

4.9 Evaluation of Action Sequence Prediction

Next, we formulated the abductive action sequence prediction task based on the *Abduct at T* setup. We attached a GRU / Transformer decoder to our existing object-relational models (in Table 1). To train both sequence prediction models, we freeze the object detector and relational model ($\phi()$). Then, we use the relational vector x_r and action distribution obtained from $\phi_c()$ in Eq. 3 as the initial hidden state and pass it to the GRU respectively. The transformer decoder takes non-pooled relational features (a matrix of size $n \times d$) as the key, value, and max-pooled relational features x_r as the query. The output of these models is fed into a linear classifier to produce action sequences autoregressively. The results of these models are reported in Table 3. The BiGED model obtains slightly better performance than the rest. Although the performances of these models are suboptimal, we note that humans are also unable to obtain satisfactory results (only 14.00% accuracy). As we are constrained to only utilize available information in a single frame, the solution contains a substantial amount of sequence permutations. Therefore, the task is extremely challenging. The poor human performance also suggests how humans may use abduction. Perhaps humans do not resolve causal chains when performing abduction as it is a very challenging task.

4.10 Evaluation of Abductive Action Verification

We present abductive action verification results in Table 4 using the object-relational approach. We use the ground truth human and object class names to obtain the semantic representation. As the query is in textual form (i.e. the action class name), we suggest that the abductive action verification resembles a human-like task. It is easy to answer yes, or no to the question "Did the person execute action a_i in this snapshot to arrive at this state?" Interestingly, the performance of this task is slightly lower than the main results we

obtained in Table 1. Even though this task is mentally more straightforward for the human, it seems the task is slightly difficult for the machine as it now has to understand the complexities of human languages.

4.11 Qualitative Results

We compare qualitative results for the abductive action set prediction task in Figure 9. Depending on the number of past action labels a snapshot has, we take the same number of top-k predicted actions from each model. All models demonstrate their ability to perform abductive action inference. In the first snapshot, there are objects such as a person, laptop, table, cup, and dish. In the second snapshot, there are objects such as a person, floor, blanket, bag, and vacuum. In both scenarios, RBP and BiGED demonstrate that they can infer actions more accurately.

4.12 Object-Relational Model Parameters

The proposed object-relational model parameters are shown in Table 5. The Rule-based Inference (RI) model does not have any parameters and is therefore omitted from the table. Based on the results shown earlier, we note that the Graph Neural Network Encoder Decoder (GNNED) model obtains better performance than the Transformer model even though it has lesser parameters. In addition, our proposed Bilinear Graph Encoder Decoder (BiGED) model has lesser parameters and performs comparable to or better than the Relational Bilinear pooling (RBP) model. These further demonstrate the effectiveness of the proposed GNNED, RBP, and BiGED models for the challenging task of abductive action inference.

4.13 Ablation Study

Ablation on graph affinity function: By default, we use the Jaccard Vector Similarity as the affinity $W_A(i, j)$ for the GNNED and BiGED models. Here, we ablate the impact of this design choice by comparing it with cosine similarity and dot product. As can be seen from the results in Table 6, the Jaccard Vector Similarity (JVS) obtains better results than cosine similarity and dot product. This behavior can be attributed to the fully differentiable and bounded nature of JVS compared to dot product or the cosine similarity.

Impact of semantic features and learning scheduler: Apart from the two different setups mentioned, we also use a third setup for ablations. In the third

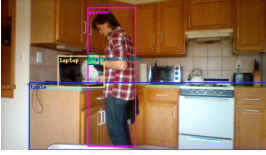
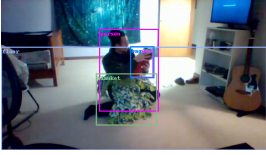
Snapshot	MLP	Transformer	GNNED	RBP	BiGED
	Holding a dish Taking a cup/glass/bottle from somewhere Holding a cup/glass/bottle of something Working/Playing on a laptop Working at a table Watching a laptop or something on a laptop Drinking from a cup/glass/bottle	Holding a dish Taking a cup/glass/bottle from somewhere Holding a cup/glass/bottle of something Working/Playing on a laptop Working at a table Watching a laptop or something on a laptop Drinking from a cup/glass/bottle	Holding a dish Taking a cup/glass/bottle from somewhere Holding a cup/glass/bottle of something Working/Playing on a laptop Working at a table Watching a laptop or something on a laptop Drinking from a cup/glass/bottle	Holding a dish Taking a cup/glass/bottle from somewhere Holding a cup/glass/bottle of something Working/Playing on a laptop Working at a table Watching a laptop or something on a laptop Drinking from a cup/glass/bottle	Holding a dish Taking a cup/glass/bottle from somewhere Holding a cup/glass/bottle of something Working/Playing on a laptop Working at a table Watching a laptop or something on a laptop Drinking from a cup/glass/bottle
	Holding a blanket Holding a bag Snuggling with a blanket Sitting on the floor Lying on the floor Holding a vacuum Someone is awakening somewhere	Holding a blanket Holding a bag Snuggling with a blanket Sitting on the floor Lying on the floor Holding a vacuum Someone is awakening somewhere	Holding a blanket Holding a bag Snuggling with a blanket Sitting on the floor Lying on the floor Holding a vacuum Someone is awakening somewhere	Holding a blanket Holding a bag Snuggling with a blanket Sitting on the floor Lying on the floor Holding a vacuum Someone is awakening somewhere	Holding a blanket Holding a bag Snuggling with a blanket Sitting on the floor Lying on the floor Holding a vacuum Someone is awakening somewhere

Figure 9: Qualitative results produced by each model on the Abductive action set inference *Abduct last snapshot* setup on the AG test dataset. The first column shows the snapshot. The remaining columns show the actions predicted by each model. Actions highlighted in green are correctly inferred while the rest are ground truth actions that the model did not infer.

Table 5: The object-relational model parameters for the abductive action inference task.

Model	Parameters
Relational MLP	13.4M
Relational Self Att. Transformer	101.2M
Relational Cross Att. Transformer	65.9M
Relational GNNED	80.7M
RBP	373.4M
BiGED	213.6M

Table 6: Ablation on graph affinity using *Abduct at T* setup.

Model	mAP	R@10	mR@10
Jaccard Vector Similarity	35.75	60.55	44.37
Cosine Similarity	34.17	57.98	41.97
Dot product	28.81	54.68	38.38

setup, the action sets are formed from the current and previous snapshots which form the ground truth denoted by $\mathcal{A} = \{\mathcal{A}_{t-1} \cup \mathcal{A}_t\}$ for faster experimentation. We retrain all object-relational models with the corresponding past action set obtained from the current and previous snapshots. We perform ablation studies on the relational self-attention Transformer based on this setup. These findings can also be generalized to

Table 7: Ablation study for the impact of semantic features and scheduler on the abductive action set inference for the *Abduct from current and previous snapshot* setup using self-attention Transformer.

Model	mAP	R@10	mR@10
Visual only	21.42	46.44	34.24
Visual + scheduler	21.93	47.04	34.80
Visual + semantic	35.40	68.47	54.90
Visual + semantic + scheduler	35.77	69.16	55.70

the other setups as mentioned earlier.

We evaluate the effect of visual and semantic (Glove [35]) features in Table 7. The use of semantic features provides a huge performance boost across all metrics. We attribute the performance increase to the contextual information provided by the semantics. The semantics of objects enables the model to identify and relate the actions effectively and provide an easier means to reason about actions. It is also interesting to see the impact of the learning rate scheduler which provides considerable improvement for the Transformer model. Therefore, we use semantics and the learning rate scheduler for all our models.

5 Discussion & Conclusion

This paper introduced a new task called abductive action inference which comprises an action set prediction, action sequence prediction, and abductive action verification. Our experiments demonstrate that deep learning models are able to perform abductive action inference to a certain extent. Moreover, we showed that end-to-end trained holistic representational models are not effective in this task. In addition, although large-scale multi-modal foundational models such as CLIP [31] show some promising results, our proposed human-object relational modeling methods such as relational graph neural networks, relational bilinear pooling and their combination, BiGED outperform these existing models. This reveals the effectiveness of object-relational models for abductive action inference. Our investigation also shows that GPT-3.5 models are either overly conservative or aggressive for the abductive action inference task. Therefore, GPT-3.5 was unable to achieve comparable results compared to CLIP or other object-relational methods. Abductive action inference presents a challenging AI research problem. Therefore, we believe this research question deserves further investigation. In the future, we plan to extend abduction inference to abductive event inference where given a state, the objective is to infer past events.

Acknowledgment This research/project is supported by the National Research Foundation, Singapore, under its NRF Fellowship (Award NRF-NRFF14-2022-0001). Any opinions, findings and conclusions or recommendations expressed in this material are those of the author(s) and do not reflect the views of the National Research Foundation, Singapore.

References

- [1] C. Liang, W. Wang, T. Zhou, and Y. Yang, "Visual abductive reasoning," in *Proceedings of the IEEE/CVF Conference on Computer Vision and Pattern Recognition*, 2022, pp. 15 565–15 575.
- [2] J. Hessel, J. D. Hwang, J. S. Park, R. Zellers, C. Bhagavatula, A. Rohrbach, K. Saenko, and Y. Choi, "The abduction of sherlock holmes: A dataset for visual abductive reasoning," *arXiv preprint arXiv:2202.04800*, 2022.
- [3] H. Jhuang, J. Gall, S. Zuffi, C. Schmid, and M. J. Black, "Towards understanding action recognition," in *Proceedings of the IEEE international conference on computer vision*, 2013, pp. 3192–3199.
- [4] S. Herath, M. Harandi, and F. Porikli, "Going deeper into action recognition: A survey," *Image and vision computing*, vol. 60, pp. 4–21, 2017.
- [5] G. Guo and A. Lai, "A survey on still image based human action recognition," *Pattern Recognition*, vol. 47, no. 10, pp. 3343–3361, 2014.
- [6] A. Furnari and G. M. Farinella, "What would you expect? anticipating egocentric actions with rolling-unrolling lstms and modality attention," in *Proceedings of the IEEE/CVF International Conference on Computer Vision*, 2019, pp. 6252–6261.
- [7] B. Fernando and S. Herath, "Anticipating human actions by correlating past with the future with jaccard similarity measures," in *Proceedings of the IEEE/CVF Conference on Computer Vision and Pattern Recognition*, 2021, pp. 13 224–13 233.
- [8] Y. Abu Farha, A. Richard, and J. Gall, "When will you do what?-anticipating temporal occurrences of activities," in *Proceedings of the IEEE conference on computer vision and pattern recognition*, 2018, pp. 5343–5352.
- [9] T. Han, W. Xie, and A. Zisserman, "Video representation learning by dense predictive coding," in *Proceedings of the IEEE/CVF International Conference on Computer Vision Workshops*, 2019, pp. 0–0.
- [10] R. Girdhar and K. Grauman, "Anticipative video transformer," in *Proceedings of the IEEE/CVF International Conference on Computer Vision*, 2021, pp. 13 505–13 515.
- [11] R. Zellers, Y. Bisk, A. Farhadi, and Y. Choi, "From recognition to cognition: Visual commonsense reasoning," in *Proceedings of the IEEE/CVF conference on computer vision and pattern recognition*, 2019, pp. 6720–6731.
- [12] A. Wu, L. Zhu, Y. Han, and Y. Yang, "Connective cognition network for directional visual commonsense reasoning," *Advances in Neural Information Processing Systems*, vol. 32, 2019.
- [13] J. S. Park, C. Bhagavatula, R. Mottaghi, A. Farhadi, and Y. Choi, "Visualcomet: Reasoning about the dynamic context of a still image," in *European Conference on Computer Vision*. Springer, 2020, pp. 508–524.
- [14] W.-Z. Dai, Q. Xu, Y. Yu, and Z.-H. Zhou, "Bridging machine learning and logical reasoning by abductive learning," *Advances in Neural Information Processing Systems*, vol. 32, 2019.
- [15] T. Zhong, Y. Wei, L. Yang, Z. Wu, Z. Liu, X. Wei, W. Li, J. Yao, C. Ma, X. Li *et al.*, "Chatabl: Abductive learning via natural language interaction with chatgpt," *arXiv preprint arXiv:2304.11107*, 2023.
- [16] L.-W. Cai, W.-Z. Dai, Y.-X. Huang, Y.-F. Li, S. H. Muggleton, and Y. Jiang, "Abductive learning with ground knowledge base." in *IJCAI*, 2021, pp. 1815–1821.
- [17] Z. Han, L.-W. Cai, W.-Z. Dai, Y.-X. Huang, B. Wei, W. Wang, and Y. Yin, "Abductive subconcept learning," *Science China Information Sciences*, vol. 66, no. 2, p. 122103, 2023.

- [18] Y. Jin, L. Zhu, and Y. Mu, “Complex video action reasoning via learnable markov logic network,” in *Proceedings of the IEEE/CVF Conference on Computer Vision and Pattern Recognition*, 2022, pp. 3242–3251.
- [19] W. Zhao, Y. Rao, Y. Tang, J. Zhou, and J. Lu, “Videoabc: A real-world video dataset for abductive visual reasoning,” *IEEE Transactions on Image Processing*, vol. 31, pp. 6048–6061, 2022.
- [20] K. Tang, Y. Niu, J. Huang, J. Shi, and H. Zhang, “Un-biased scene graph generation from biased training,” in *Proceedings of the IEEE/CVF conference on computer vision and pattern recognition*, 2020, pp. 3716–3725.
- [21] Y. Cong, W. Liao, H. Ackermann, B. Rosenhahn, and M. Y. Yang, “Spatial-temporal transformer for dynamic scene graph generation,” in *Proceedings of the IEEE/CVF International Conference on Computer Vision*, 2021, pp. 16 372–16 382.
- [22] M. Yatskar, L. Zettlemoyer, and A. Farhadi, “Situation recognition: Visual semantic role labeling for image understanding,” in *Proceedings of the IEEE conference on computer vision and pattern recognition*, 2016, pp. 5534–5542.
- [23] F. Scarselli, M. Gori, A. C. Tsoi, M. Hagenbuchner, and G. Monfardini, “The graph neural network model,” *IEEE transactions on neural networks*, vol. 20, no. 1, pp. 61–80, 2008.
- [24] C. Yu, Y. Liu, C. Gao, C. Shen, and N. Sang, “Representative graph neural network,” in *European Conference on Computer Vision*. Springer, 2020, pp. 379–396.
- [25] M. Schlichtkrull, T. N. Kipf, P. Bloem, R. v. d. Berg, I. Titov, and M. Welling, “Modeling relational data with graph convolutional networks,” in *European semantic web conference*. Springer, 2018, pp. 593–607.
- [26] Y. Gao, O. Beijbom, N. Zhang, and T. Darrell, “Compact bilinear pooling,” in *Proceedings of the IEEE Conference on Computer Vision and Pattern Recognition (CVPR)*, June 2016.
- [27] A. Fukui, D. H. Park, D. Yang, A. Rohrbach, T. Darrell, and M. Rohrbach, “Multimodal compact bilinear pooling for visual question answering and visual grounding,” *arXiv preprint arXiv:1606.01847*, 2016.
- [28] J. Johnson, B. Hariharan, L. Van Der Maaten, J. Hoffman, L. Fei-Fei, C. Lawrence Zitnick, and R. Girshick, “Inferring and executing programs for visual reasoning,” in *Proceedings of the IEEE international conference on computer vision*, 2017, pp. 2989–2998.
- [29] S. Subramanian, M. Narasimhan, K. Khangaonkar, K. Yang, A. Nagrani, C. Schmid, A. Zeng, T. Darrell, and D. Klein, “Modular visual question answering via code generation,” *arXiv preprint arXiv:2306.05392*, 2023.
- [30] C. Feichtenhofer, H. Fan, J. Malik, and K. He, “Slow-fast networks for video recognition,” in *Proceedings of the IEEE/CVF international conference on computer vision*, 2019, pp. 6202–6211.
- [31] A. Radford, J. W. Kim, C. Hallacy, A. Ramesh, G. Goh, S. Agarwal, G. Sastry, A. Askell, P. Mishkin, J. Clark *et al.*, “Learning transferable visual models from natural language supervision,” in *International conference on machine learning*. PMLR, 2021, pp. 8748–8763.
- [32] J. Li, D. Li, C. Xiong, and S. Hoi, “Blip: Bootstrapping language-image pre-training for unified vision-language understanding and generation,” in *International Conference on Machine Learning*. PMLR, 2022, pp. 12 888–12 900.
- [33] S. Ren, K. He, R. Girshick, and J. Sun, “Faster r-cnn: Towards real-time object detection with region proposal networks,” *Advances in neural information processing systems*, vol. 28, 2015.
- [34] K. He, X. Zhang, S. Ren, and J. Sun, “Deep residual learning for image recognition,” in *Proceedings of the IEEE conference on computer vision and pattern recognition*, 2016, pp. 770–778.
- [35] J. Pennington, R. Socher, and C. D. Manning, “Glove: Global vectors for word representation,” in *Proceedings of the 2014 conference on empirical methods in natural language processing (EMNLP)*, 2014, pp. 1532–1543.
- [36] A. Vaswani, N. Shazeer, N. Parmar, J. Uszkoreit, L. Jones, A. N. Gomez, L. Kaiser, and I. Polosukhin, “Attention is all you need,” *Advances in neural information processing systems*, vol. 30, 2017.
- [37] J. L. Ba, J. R. Kiros, and G. E. Hinton, “Layer normalization,” *arXiv preprint arXiv:1607.06450*, 2016.
- [38] A. Radford, K. Narasimhan, T. Salimans, I. Sutskever *et al.*, “Improving language understanding by generative pre-training,” 2018.
- [39] A. Radford, J. Wu, R. Child, D. Luan, D. Amodei, I. Sutskever *et al.*, “Language models are unsupervised multitask learners,” *OpenAI blog*, vol. 1, no. 8, p. 9, 2019.
- [40] T. Brown, B. Mann, N. Ryder, M. Subbiah, J. D. Kaplan, P. Dhariwal, A. Neelakantan, P. Shyam, G. Sastry, A. Askell *et al.*, “Language models are few-shot learners,” *Advances in neural information processing systems*, vol. 33, pp. 1877–1901, 2020.
- [41] J. Ji, R. Krishna, L. Fei-Fei, and J. C. Niebles, “Action genome: Actions as compositions of spatio-temporal scene graphs,” in *Proceedings of the IEEE/CVF Conference on Computer Vision and Pattern Recognition*, 2020, pp. 10 236–10 247.
- [42] G. A. Sigurdsson, G. Varol, X. Wang, A. Farhadi, I. Laptev, and A. Gupta, “Hollywood in homes: Crowdsourcing data collection for activity understanding,” in *European Conference on Computer Vision*. Springer, 2016, pp. 510–526.

- [43] I. Loshchilov and F. Hutter, “Decoupled weight decay regularization,” *arXiv preprint arXiv:1711.05101*, 2017.
- [44] A. Dosovitskiy, L. Beyer, A. Kolesnikov, D. Weissenborn, X. Zhai, T. Unterthiner, M. Dehghani, M. Minderer, G. Heigold, S. Gelly *et al.*, “An image is worth 16x16 words: Transformers for image recognition at scale,” *arXiv preprint arXiv:2010.11929*, 2020.
- [45] O. Russakovsky, J. Deng, H. Su, J. Krause, S. Satheesh, S. Ma, Z. Huang, A. Karpathy, A. Khosla, M. S. Bernstein, A. C. Berg, and L. Fei-Fei, “Imagenet large scale visual recognition challenge,” *CoRR*, vol. abs/1409.0575, 2014. [Online]. Available: <http://arxiv.org/abs/1409.0575>
- [46] W. Kay, J. Carreira, K. Simonyan, B. Zhang, C. Hillier, S. Vijayanarasimhan, F. Viola, T. Green, T. Back, P. Natsev *et al.*, “The kinetics human action video dataset,” *arXiv preprint arXiv:1705.06950*, 2017.